

Journal Pre-proofs

Research paper

Dinuclear mixed valence cobalt(II/III) and hetero-tetranuclear cobalt(III)/Na complexes with a compartmental ligand: Synthesis, characterization and use as catalysts for oxidative dimerisation of 2-aminophenol

Abhisek Banerjee, Shouvik Chattopadhyay

PII: S0020-1693(20)31244-5
DOI: <https://doi.org/10.1016/j.ica.2020.120044>
Reference: ICA 120044

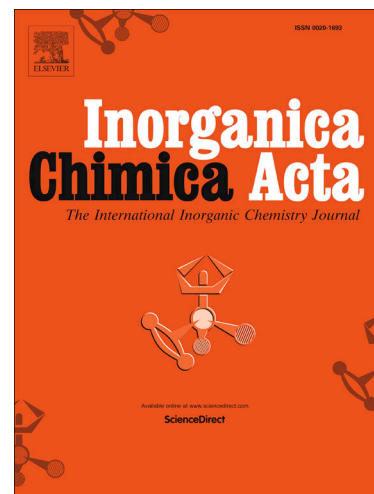
To appear in: *Inorganica Chimica Acta*

Received Date: 22 July 2020
Revised Date: 23 September 2020
Accepted Date: 23 September 2020

Please cite this article as: A. Banerjee, S. Chattopadhyay, Dinuclear mixed valence cobalt(II/III) and hetero-tetranuclear cobalt(III)/Na complexes with a compartmental ligand: Synthesis, characterization and use as catalysts for oxidative dimerisation of 2-aminophenol, *Inorganica Chimica Acta* (2020), doi: <https://doi.org/10.1016/j.ica.2020.120044>

This is a PDF file of an article that has undergone enhancements after acceptance, such as the addition of a cover page and metadata, and formatting for readability, but it is not yet the definitive version of record. This version will undergo additional copyediting, typesetting and review before it is published in its final form, but we are providing this version to give early visibility of the article. Please note that, during the production process, errors may be discovered which could affect the content, and all legal disclaimers that apply to the journal pertain.

© 2020 Elsevier B.V. All rights reserved.



Dinuclear mixed valence cobalt(II/III) and heterotetranuclear cobalt(III)/Na complexes with a compartmental ligand: Synthesis, characterization and use as catalysts for oxidative dimerisation of 2-aminophenol

Abhisek Banerjee, Shouvik Chattopadhyay*

Department of Chemistry, Inorganic Section, Jadavpur University, Kolkata - 700032, India.

Tel: +9133-2457-2941; E-mail: shouvik.chem@gmail.com

Abstract

A N_2O_4 donor compartmental reduced Schiff base ligand, H_2L [(2,2-dimethyl-1,3-propanediyl)bis(iminomethylene)bis(6-methoxyphenol)], obtained on 1:2 condensation of 2,2-dimethyl-1,3-propanediamine with *ortho*-vanillin followed by reduction with $NaBH_4$ in methanol solution, has been used to prepare two cobalt complexes, $[(N_3)Co^{III}L(\mu-OAc)Co^{II}(N_3)]$ (**1**) and $[(\mu-N_3)_2\{(AcO)Co^{III}LNa(CH_3OH)\}_2] \cdot 2CH_3OH$ (**2**). Complex **1** is a dinuclear mixed valence cobalt(III)/cobalt(II) complex with $Co^{III}O_2Co^{II}$ core. Complex **2**, on the other hand, is a tetranuclear cobalt(III)/sodium complex with $CoO_2Na(N_3)_2NaO_2Co$ core. Formation of complex **1** or **2** is mainly governed by the amount of cobalt(II) precursors present in the reaction mixture. Each complex has been characterized by elemental and spectral analysis. X-ray diffraction analysis has confirmed their structures. Complex **1** crystallized in a chiral space group $Pna2_1$ where both the cobalt(III) and cobalt(II) centers adopt six-coordinate distorted octahedral geometry with cobalt(III) and cobalt(II) centers residing respectively at inner N_2O_2 and outer O_4

cavities of the reduced Schiff base. Complex **2** crystallized in triclinic system with $P\bar{1}$ space group, where both cobalt(III) and sodium centers adopt distorted octahedral geometry. Oxidation states of cobalt centers have been confirmed by bond length consideration, BVS calculations as well as from room temperature magnetic moment measurement. Both complexes **1** and **2** show phenoxazinone synthase mimicking activity with k_{cat} values 250.21 and 493.73 h^{-1} respectively.

1. Introduction

3d metal mixed valence complexes have sparked large interests owing to their potential application in molecular electronics and molecular computing [1-4]. The most renowned mixed valence complex of cobalt is Co_3O_4 , a normal spinel, where the cobalt(III) centers are octahedral and low spin, whereas cobalt(II) centers are tetrahedral and high spin [5]. The mixed valence cobalt complexes are less common in literature compared to manganese and iron, and therefore their importance in catalysis, magnetism and electro-chromism is less explored [6-8]. Recently, synthetic inorganic chemists are trying to synthesize mixed valence cobalt(II/III) complexes via partial oxidation of cobalt(II) precursors and some di and trinuclear mixed valence cobalt(II/III) complexes are reported in literature [9-18].

The synthetic inorganic chemists are also attracted in the field of synthesis, characterization of heteronuclear complexes containing alkali metal ions for their wide range of applications since long [19-23]. Recent example of sodium mediated electron transfer reactions between the two metal salicylaldimine species in $[\text{Na}\{\text{Ni}(\text{salen})\}_2]^+$ type complexes has increased this attraction [24]. The easiest way to synthesize such heteronuclear complexes is to use compartmental ligands [25-29] of which ‘salen’ based N_2O_4 donor compartmental Schiff base ligands are the most common, as their inner N_2O_2 core is suitable for accommodation of

different transition metal ions and outer O₄ core can accommodate alkali metal ions easily [30-32].

Reduction of Schiff bases with borohydride may produce ‘reduced Schiff bases’, which are better complexing agent considering their more flexibility due to the absence of imine (>C=N) functionality [33-35]. Many compartmental ‘reduced Schiff bases’ have been used by several groups to prepare mixed valence cobalt(II/III) complexes and also heteronuclear cobalt(III)/Na complexes [17-18, 31,34]. In this work, we have used a reduced Schiff base to prepare a mixed valence cobalt(II/III) complex and also heteronuclear cobalt(III)/Na complex. The formation of two different complexes is primarily linked with the reaction condition used for the synthesis of these complexes. Both complexes were characterized by elemental and spectral analysis. Their structures were confirmed by single crystal X-ray diffraction study. The ability of both complexes to catalyze the oxidative dimerization of 2-aminophenol (i.e. phenoxazinone synthase mimicking activity) is also explored and correlated with their structures.

Herein, we would like to report the synthesis, structure and catalytic ability of two cobalt complexes with a compartmental N₂O₄ donor ‘reduced Schiff base’.

Keywords: Cobalt, mixed valence, compartmental ligand, phenoxazinone synthase.

2. Experimental Section

Materials

All chemicals used were purchased from Sigma-Aldrich and were of reagent grade. They were used without further purification.

2.1. Synthesis

2.1.1. Synthesis of a reduced Schiff base ligand, H_2L [(2,2-dimethyl-1,3-propanediyl)bis(iminomethylene)bis(6-methoxyphenol)]

2 mmol of *ortho*-vanillin (304 mg) was mixed with 1 mmol of 2,2-dimethyl-1,3-propanediamine (0.12 mL) in 10 ml methanol and the resulting solution was allowed to reflux for ca. 2 hr. to synthesize the hexadentate Schiff base ligand, H_2L^a {[*N,N'*-bis(3-ethoxysalicylidene)2,2-dimethyl-1,3-propanediamine]}. Then this prepared Schiff base solution was cooled to 0°C, followed by the addition of 4 mmol solid sodium borohydride (150 mg) to it with constant stirring. After completion of sodium borohydride addition the resulting solution was acidified with 10 mL glacial acetic acid and placed under reduced pressure in a rotary evaporator maintaining the temperature to ~60°C. The residue was dissolved finally in minimum volume of water and extracted with 15 mL of dichloromethane using a separating funnel. The ligand solution in dichloromethane was dried using anhydrous sodium acetate and then dichloromethane was evaporated under reduced pressure and the ligand, H_2L , was extracted in methanol. The ligand was not isolated and the methanol solution was used directly for the synthesis of complexes **1** and **2**.

2.2. Synthesis of the complexes

2.2.1. Synthesis of [$(N_3)Co^{III}L(\mu-OAc)Co^{II}(N_3)$] (**1**)

10 mL methanol solution of 2 mmol cobalt(II) acetate tetrahydrate (500 mg) was added to the methanol solution (10 mL) of the reduced Schiff base ligand, H_2L , with constant stirring for ca. 1 hr. 10 mL methanol/water solution (4:1 ratio) of 4 mmol sodium azide (260 mg) was then added to it and stirring was continued for about 2 h more. Few drops of triethylamine were added into the final solution and stirring was continued for about 1 hr. Dark brown crystals were

appeared after 4-6 days on slow evaporation of the filtrate in an open atmosphere. X-ray quality single crystals were collected from the product.

Yield: 392 mg (~62%, based on cobalt). Anal. Calc. for $C_{23}H_{31}Co_2N_8O_6$ (FW = 633.42): C, 43.57; H, 4.89; N, 17.68 %. Found: C, 43.5; H, 4.8; N, 17.8 %. FT-IR (KBr, cm^{-1}): 3195 (ν_{N-H}), 2935-2848 (ν_{C-H}), 2056(ν_{N_3}), 2035 (ν_{N_3}), 1562-1480 (ν_{COO}). UV-Vis, λ_{max} (nm), [ϵ_{max} ($L\ mol^{-1}\ cm^{-1}$)] (CH_3CN), 620 (2.01×10^2), 362 (2.03×10^3), 245 (9.5×10^3), Magnetic moment, $\mu = 5.17$ B.M.

2.2.2. Synthesis of $[(\mu-N_3)_2\{(AcO)Co^{III}LNa(CH_3OH)\}_2] \cdot 2CH_3OH$ (**2**)

10 mL methanol solution of 1 mmol cobalt(II) acetate tetrahydrate (250 mg) was added to the methanol solution (10 mL) of the reduced Schiff base ligand, H_2L , with constant stirring for ca. 1 hr. 10 mL methanol/water solution (4:1 ratio) of 4 mmol sodium azide (260 mg) was then added to it. Dark brown crystals were appeared after 4-6 days on slow evaporation of the filtrate in an open atmosphere. X-ray quality single crystals were collected from the product.

Yield: 340 mg (~55%, based on cobalt). Anal. Calc. for $C_{50}H_{76}Co_2N_{10}Na_2O_{16}$ (FW =1237.05): C, 48.50; H, 6.14; N, 11.31 %. Found: C, 48.4; H, 6.1; N, 11.4 %. FT-IR (KBr, cm^{-1}): 3210 (ν_{N-H}), 2960-2885 (ν_{C-H}), 2051 (ν_{N_3}), 1577-1485 (ν_{COO}). UV-Vis, λ_{max} (nm), [ϵ_{max} ($dm^3\ mol^{-1}\ cm^{-1}$)] (CH_3CN), 706 (1.05×10^2), 352 (3.80×10^3), 255 (8.1×10^3), Diamagnetic.

2.3. Physical measurements

Elemental analyses (carbon, hydrogen and nitrogen) were performed using a Perkin Elmer 240C elemental analyzer. IR spectra in KBr ($4500-500\ cm^{-1}$) were recorded with a Perkin Elmer Spectrum Two spectrophotometer. Electronic spectra in acetonitrile (800-200 nm) were

recorded on a Perkin Elmer Lambda 35 UV-visible spectrophotometer. The magnetic susceptibility measurement was done with an EG & PAR vibrating sample magnetometer (Model 155) at 25 °C and diamagnetic corrections were performed using Pascal's constants.

Molar conductivity measurements were performed on a Jencons 4010 Conductivity Meter in nitrobenzene at 25 °C.

2.4. X-ray crystallography

Suitable single crystals of both complexes were used for data collection using a 'Bruker D8 QUEST area detector' diffractometer equipped with graphite-monochromated Mo K α radiation ($\lambda = 0.71073 \text{ \AA}$). The molecular structures were solved by direct method and refined by full-matrix least squares on F^2 using the SHELXL-14 package [36]. Non-hydrogen atoms were refined with anisotropic thermal parameters. Hydrogen atoms attached to nitrogen and oxygen atoms were located by difference Fourier maps and were kept at fixed positions. All other hydrogen atoms were placed in their geometrically idealized positions and constrained to ride on their parent atoms. Multi-scan empirical absorption corrections were applied to the data using the program SADABS [37]. In complex **1**, three carbon atoms (C8, C37 and C38) have been refined as isotropic only. The poor quality of the crystals of **1** gave rise to misshapen large spots in the diffraction pattern which in turn led to high R values. A summary of the crystallographic data has been given in Table S1 (Supplementary Information). Selected bond lengths have been listed in Tables 2 (Unit-I of complex **1** and complex **2**) and S2 (Unit-II of complex **1**). Bond angles of both complexes have been given in Table S3.

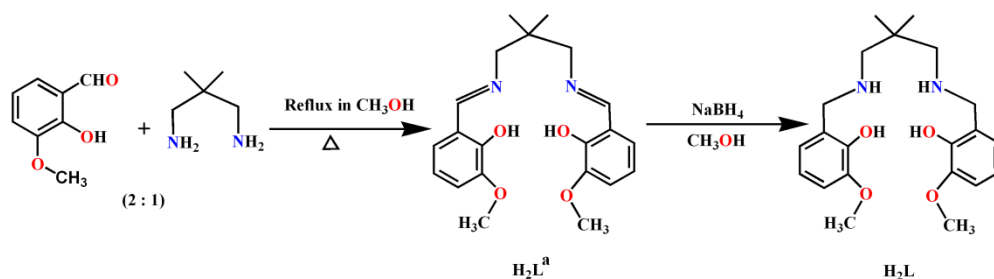
2.5. Kinetics of the phenoxazinone synthase activity

The phenoxazinone synthase (PHS) mimicking activity of both complexes has been checked by monitoring the oxidation of 2-aminophenol (2-AP) spectrophotometrically in acetonitrile medium at 25 °C. Every catalytic reaction has been studied spectrophotometrically for ca. 2 h in the wavelength range 300-600 nm. Before entering into to the kinetic study in detail, it is mandatory to check the ability of these complexes to behave as a catalyst for carrying out the oxidation of 2-aminophenol. Thus 1.0×10^{-4} M solutions of the complexes have been treated with a 0.01 M solution of 2-aminophenol, and the spectra have been recorded in acetonitrile medium at 25°C. The steady increase in the absorbance as a function of time at ca. 433 nm, is the characteristic of its corresponding chromophore, 2-aminophenoxazin-3-one. Furthermore, the catalytic rate dependency on concentration of catalyst has been monitored by performing similar sets of experiments at a fixed concentration of substrate with variable catalyst concentrations. Rate of the reactions have been calculated from the initial rate method, and the average initial rate over three independent measurements was also recorded. One thing must be emphasized here that a blank experiment without catalyst (only complex) has been carried out in an identical reaction condition and does not show significant growth of the band at ~ 433 nm, characteristic of phenoxazinone chromophore.

3. Results and discussion

3.1. Synthesis

2,2-dimethyl-1,3-propanediamine and *ortho*-vanillin have been used to synthesize the potential hexadentate compartmental reduced Schiff base ligand, H_2L , following the literature method [31] (Scheme 1).



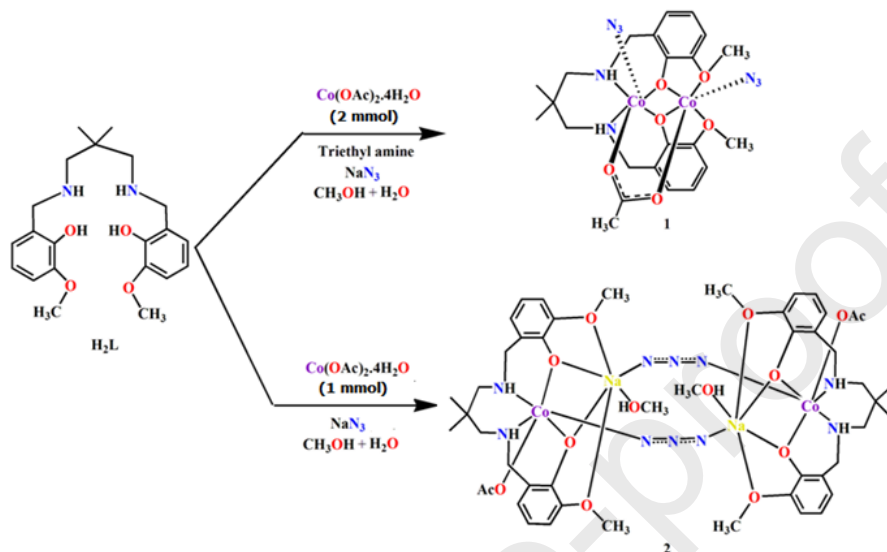
Scheme 1: Synthetic route to the reduced Schiff base ligand, H_2L .

The methanol solution of H_2L , on reaction with cobalt(II) acetate tetrahydrate followed by the addition of sodium azide in slightly alkaline medium produced a dinuclear mixed valence cobalt(III)/cobalt(II) complex, **1**. In addition, the treatment of methanol solution of H_2L with the cobalt(II) acetate tetrahydrate in presence of excess sodium azide produced a centrosymmetric tetrameric cobalt(III)/sodium complex, **2**. The synthetic routes to the complexes have been shown in Scheme 2. Cobalt(II) is definitely oxidized by areal oxidation. The inner cobalt centers in both complexes reside in the stronger field (N_3O_3) coordination environment compared to the outer cobalt center (which resides in O_5N) in complex **1**. This may be the driving force to carry out this oxidation of inner cobalt center in both complexes.

It is to be noted here that the starting materials are more or less same for the synthesis of both complexes. However, the ratio of the reactants is different. 1 mmol cobalt(II) acetate and excess sodium azide were used for the synthesis of complex **2**, whereas 2 mmol cobalt(II) acetate and excess sodium azide was used for the synthesis of complex **1**. Thus the variation in structures is primarily governed by the different amounts of cobalt salt used as precursors. H_2L is a compartmental ligand and its inner N_2O_2 cavity traps the cobalt(III) produced by the partial oxidation of cobalt(II) and outer O_4 compartment binds with the remaining cobalt(II) to form complex **1**. However, when only 1 mmol cobalt salt is added in the reaction mixture, cobalt(III)

is trapped in inner N_2O_2 compartment and outer O_4 compartment traps sodium to form complex

2.



Scheme 2: Synthetic routes to complexes **1** and **2**. Solvent methanol molecules in complex **2** have been omitted for clarity.

Table 2. Selected bond lengths (\AA) of complexes **1** (Unit-I) and **2**.

	1	2		1	2
Co(1)-N(1)	1.929(10)	1.993(4)	M(2)-O(2)	2.121(10)	2.357(3)
Co(1)-N(2)	2.048(11)	1.981(4)	M(2)-O(3)	2.394(11)	2.482(2)
Co(1)-O(1)	2.005(11)	1.908(15)	M(2)-O(4)	2.244(11)	2.508(2)
Co(1)-O(2)	1.850(8)	1.914(1)	M(2)-O(6)	2.093(10)	-
Co(1)-N(3)	1.943(12)	1.933(4)	M(2)-O(7)	-	2.389(3)
Co(1)-O(5)	1.932(9)	1.954(2)	M(2)-N(4)	1.962(11)	-
M(2)-O(1)	1.945(8)	2.317(3)	M(2)-N(5) ^a	-	2.418(3)

(M= Co in **1** and Na in **2**), Symmetry transformation^a=1-x,1-y,2-z.

The reduced Schiff base H_2L and its precursor Schiff base H_2L^a have been used previously to prepare several complexes [38-50]. In most of the cases, H_2L^a and H_2L forms multimetallic complexes, although mononuclear complexes were also formed. In one such mononuclear complex, water molecule is placed in the outer O_4 environment to form water tetramer [38]. Complexes with H_2L^a and H_2L including nuclearity of the complexes and denticity of the ligand have been listed in Table 3.

Table 3: A list of some reported complexes of H_2L^a and H_2L : Nuclearity of the complexes and denticity of the ligand

Complexes with H_2L^a			
Complex	Nuclearity of the complex	Denticity of the ligand	Reference
$[CuL^a] \cdot 2H_2O$	Mononuclear	Tetradentate	38
$[(DMSO)_2Ni(L^a)Zn(NCS)_2]$	Dinuclear	Tetradentate	39
$[CuL^aHgCl_2]$	Dinuclear	Hexadentate	40
$[(L^a)Fe(H_2O)(\mu-Htrim)(H_2O)Fe(L^a)] \cdot H_2O$	Dinuclear	Tetradentate	41
$[(MeOH)Co(L^a)Gd(NO_3)_3]$	Dinuclear	Hexadentate	42
$[Co(L^a)(\mu-AcO)_2Gd(NO_3)_2]$	Dinuclear	Hexadentate	
$[Zn(L^a)(\mu-AcO)La(thd)_2]$	Dinuclear	Hexadentate	43
$[Ni(L^a)Na(L^a)Ni(NCS)] \cdot H_2O$	Trinuclear	Hexadentate	44
$[Ni(L^a)Na(L^a)Ni(N_3)]$	Trinuclear	Hexadentate	
$[(SCN)Co(L^a)(\mu-AcO)Na]_2$	Tetranuclear	Hexadentate	45
Complexes with H_2L			

Complex	Nuclearity of the complex	Denticity of the ligand	Reference
$[(\text{SCN})\text{Cu}(\text{L})\text{Pb}(\text{SCN})]$	Dinuclear	Hexadentate	46
$[\text{Ni}_2(\text{HL})_2(\text{DMSO})_2(\text{H}_2\text{O})_2](\text{ClO}_4)_2 \cdot \text{H}_2\text{O}$	Dinuclear	Tetradentate	47
$[(\text{SCN})\text{Ni}(\text{L})(\mu\text{-OAc})\text{Pb}]$	Dinuclear	Hexadentate	48
$[\{(\text{DMSO})(\text{H}_2\text{O})\text{Ni}(\text{L})\}_2\text{Pb}](\text{ClO}_4)_2$	Trinuclear	Hexadentate	49
$(\mu\text{-N}_3)_2[(\text{H}_2\text{O})\text{Cu}(\text{L})\text{Cd}(\text{N}_3)]_2 \cdot 2\text{CH}_3\text{OH}$	Tetranuclear	Hexadentate	
$(\mu\text{-NCS})_2[\text{Cu}(\text{L})\text{Cd}(\text{SCN})]_2 \cdot 2\text{CH}_3\text{OH}$	Tetranuclear	Hexadentate	
$[(\mu\text{-dca})_2\{(\text{dca})\text{Zn}(\text{L})\text{Zn}\}_2]$	Tetranuclear	Hexadentate	50

Htrim = dianion of trimesic acid; *thd* = tetramethylheptanedionato; *dca* = dicyanamide

3.2. Description of structures

3.2.1. $[(\text{N}_3)\text{Co}^{\text{III}}\text{L}(\mu\text{-OAc})\text{Co}^{\text{II}}(\text{N}_3)]$ (**1**)

Single crystal X-ray diffraction analysis reveals that the complex **1** crystallizes in the orthorhombic space group, $Pna2_1$. There are two independent dinuclear units (I and II) with equivalent geometry in complex **1**. A perspective view of the Unit I of complex **1** is given in Figure 1 (Unit II has very similar molecular structure: Figure S1, Supplementary Information). This complex falls under the example of mixed valence category containing both cobalt(II) and cobalt(III) centers in the neutral dinuclear core which can be confirmed by total charge balance considerations, inter-atomic cobalt-nitrogen and cobalt-oxygen distances and BVS (bond valence sum) calculations [51-56].

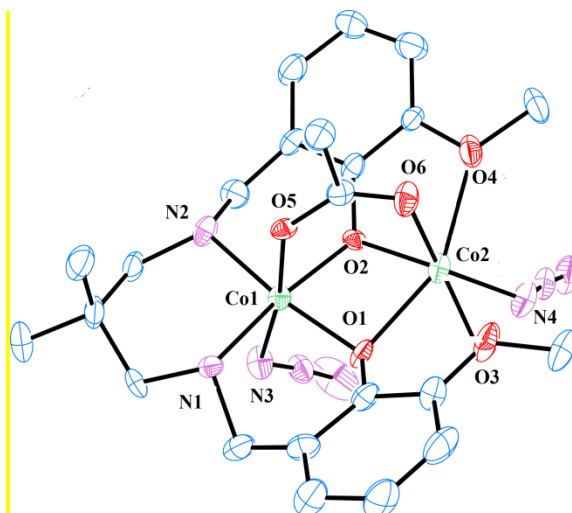


Figure 1: ORTEP view of complex **1** with 30% thermal ellipsoid probability. Hydrogen atoms have been omitted for clarity.

Cobalt(III) center, Co(1), and cobalt(II) center, Co(2) occupy the inner N_2O_2 and outer O_4 cavities respectively of the reduced Schiff base unit, H_2L . Co(1) is equatorially coordinated by two amine nitrogen atoms and two phenoxo oxygen atoms, {N(1), N(2), O(1) and O(2)} and Co(2) is equatorially coordinated by two phenoxo oxygen atoms and two methoxy oxygen atoms, {O(1), O(2), O(3) and O(4)}. The fifth coordination sites of Co(1) and Co(2) are coordinated by nitrogen atoms N(3) and N(4) respectively from two terminal azides. The oxygen atoms, O(5) and O(6), of a bridging acetate are bonded to the sixth coordination sites of Co(1) and Co(2) respectively to complete their distorted octahedral geometries. The intramolecular separation between Co(1) and Co(2) is close to 2.95 Å which is not satisfactorily short to infer any metal–metal bonding [57-58]. The saturated six membered chelate ring, Co(1)-N(1)-C(9)-C(10)-C(13)-N(2) represents chair conformation (Figure 2) with puckering parameters [59], $q(2) = 0.551(14)\text{Å}$, and $\varphi = 186(6)$.

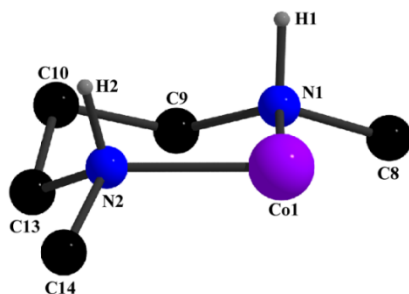


Figure 2: Chair conformation of a saturated six-membered chelating in unit-I of complex **1**. Only selected atoms have been shown.

3.2.2. $[(\mu-N_3)_2\{(AcO)Co^{III}LNa(CH_3OH)\}_2] \cdot 2CH_3OH$ (**2**)

Complex **2** is centrosymmetric and it crystallizes in the triclinic space group, $P\bar{1}$. An ORTEP view of the asymmetric unit is shown in Figure 3. In this complex, the cobalt(III) center, Co(1), occupies the inner N_2O_2 cavity and the sodium center, Na(1) occupies the outer O_4 cavity of the compartmental reduced Schiff base. Co(1) is coordinated by two amine nitrogen atoms and two phenoxo oxygen atoms, {N(1), N(2), O(1) and O(2)}, and Na(1) is coordinated by two phenoxo oxygen atoms, O(1) and O(2) and two methoxy oxygen atoms, O(3) and O(4) of the deprotonated reduced Schiff base ligands in the equatorial plane. An oxygen atom, O(5) of a terminal acetate coordinates axially to the cobalt(III) center at its fifth coordination site. The fifth coordination site of Na(1), on the other hand, is occupied by an oxygen atom, O(7) of a methanol molecule. An end to end bridging azide [(N(3)-N(4)-N(5))] connects Co(1) with a symmetry related (symmetry transformation,^a = 1-x, 1-y, 2-z) Na(1)^a to form a tetranuclear complex with $CoO_2Na(N_3)_2NaO_2Co$ core. A tentative view of the complete tetranuclear unit of complex **2** has been depicted in Figure 4.

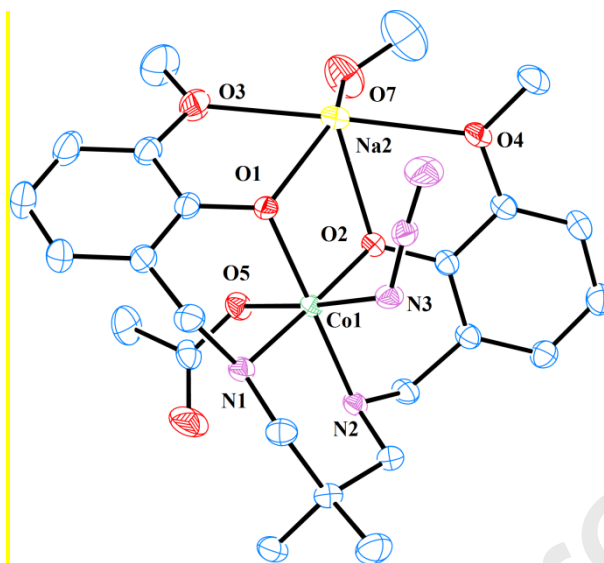


Figure 3: ORTEP view of the asymmetric unit of complex **2** with 30% thermal ellipsoid probability. Hydrogen atoms have been omitted for clarity.

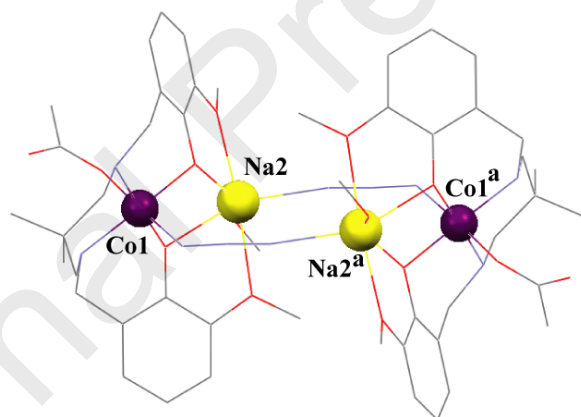


Figure 4: Perspective view of tetranuclear unit of complex **2**. Only the metal centers have been labeled here for clarity. Symmetry transformation: $a = 1-x, 1-y, 2-z$.

3.3. BVS calculation

Taking the help of bond valence sum (BVS) calculations we are able to perform the calculation of oxidation state of cobalt centers in the above prepared complexes. The results are

in good agreement for confirming the existence of mixed valence states (+2 and +3) of cobalt in complex **1** while the cobalt center in complex **2** is approximately in +3 state. Thus this bond valence sum calculative strategy is considered as one of the promising tools which strongly supports the assignment of mixed valence states of cobalt in complex **1**. The BVS values calculated for all the cobalt centers in both complexes have been listed in Table 4.

Table 4: BVS (Bond Valence Sum) values of the cobalt centers in both complexes.

Complex	Cobalt centers	BVS of cobalt
1	Co(1)	3.05
	Co(2)	1.96
	Co(3)	3.08
	Co(4)	2.05
2	Co(1)	3.03

3.4. Supramolecular interactions

In complex **1**, the hydrogen atoms, H(1) [attached to amine nitrogen atom, N(1)] and H(2) [attached to amine nitrogen atom, N(2)] are involved in intermolecular hydrogen bonding with symmetry related nitrogen atoms, N(7)^b and N(5)^b, respectively of the terminal azide groups {symmetry transformation,^b = -1/2+x, 1/2-y, 1-z} of a neighboring molecule leading to the formation of a chain like structure (Figure 5). Similar kind of interaction has been observed in Unit-II. In complex **2**, on the other hand, two hydrogen atoms, H(1) and H(2), attached to amine nitrogen atoms, N(1) and N(2), are involved in intramolecular hydrogen bonding with an oxygen atom, O(6), of the acetate group (Figure 6). The details of hydrogen bonding interactions in both complexes have been provided in Table 5.

Table 5: Hydrogen bond distances (Å) and angles (°) for complexes **1** and **2**.

Complex	D-H...A	D-H	H...A	D...A	\angle D-H...A
1	N(1)-H(1)...N(8) ^b	0.980(6)	2.470(6)	3.430(2)	164.00(1)
	N(2)-H(2)...N(7) ^b	0.980(6)	2.120(4)	3.093(4)	174.00(9)
	N(9)-H(9)...N(15) ^c	0.980(6)	2.150(4)	3.115(3)	169.00(9)
	N(9)-H(9)...N(16) ^c	0.980(6)	2.570(4)	3.530(2)	166.00(9)
2	N(1)-H(1)...O(6)	0.80(3)	2.25(3)	2.962(3)	149.00(3)
	N(2)-H(2)...O(6)	0.85(3)	2.28(3)	3.039(3)	150.00(3)

D = donor; H = hydrogen; A = acceptor, Symmetry transformation:^b= $-1/2+x, 1/2-y, 1-z$, ^c= $1/2+x, 3/2-y, z$.

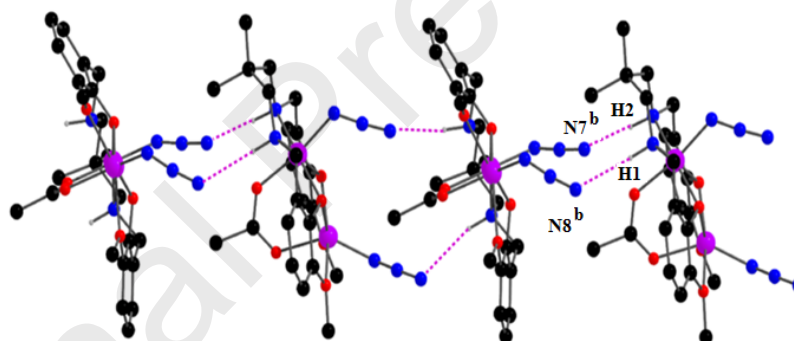


Figure 5: Perspective view of a chain structure through intermolecular hydrogen bonding interactions in Unit-I of complex **1**. Only relevant atoms have been shown here for clarity. Symmetry transformation:^b= $1/2+x, 1/2-y, 1-z$.

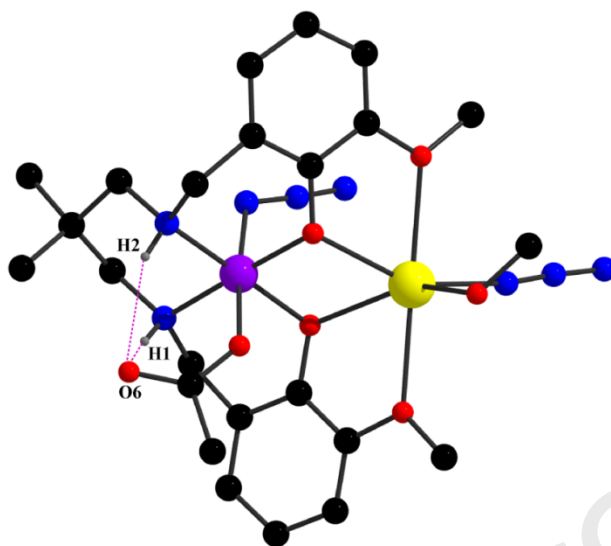


Figure 6: Perspective view of intramolecular hydrogen bonding interactions in complex **2**. Only a dinuclear fragment of the complex and only relevant atoms have been shown here for clarity.

3.5. Hirshfeld surface analyses

Hirshfeld surface analysis has been accomplished in order to examine thoroughly the strength and role of hydrogen bonds and other intermolecular contacts, and to estimate their importance for the crystal lattice stability. The Hirshfeld surfaces of both complexes have been mapped over d_{norm} (range -0.1 \AA to 1.5 \AA); shape index and curvedness (Figure 7). Graphical plots of the molecular Hirshfeld surfaces mapped with d_{norm} used a red-white-blue colour scheme, where red highlights shorter contacts, white is used for contacts around the Van der Waals separation, and blue is for longer contacts. The intense circular depressions (deep red) seen on the surfaces is indicative of hydrogen bonding contacts whereas small extent of area and light colour on the surface indicates weaker and longer contact other than hydrogen bonds.

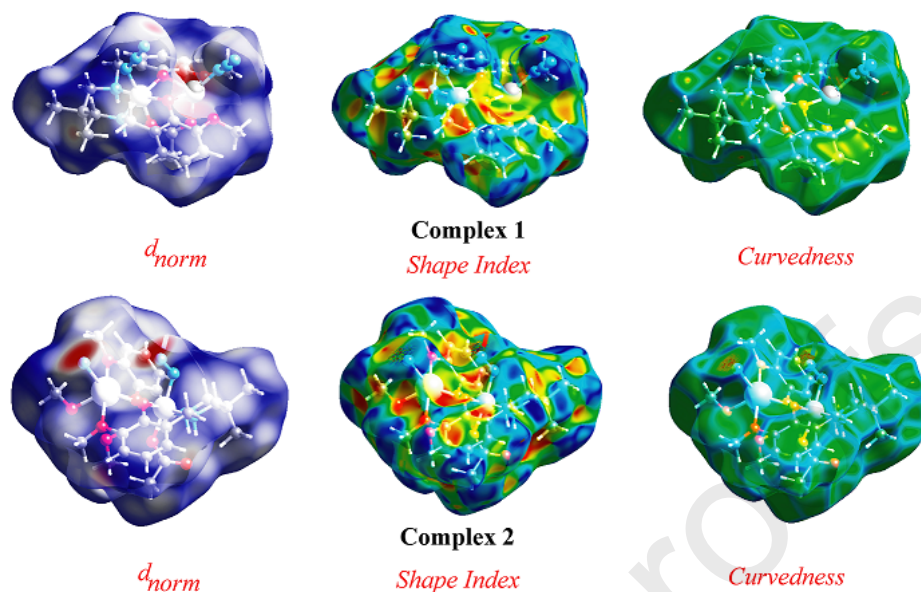


Figure 7: Hirshfeld surfaces mapped with d_{norm} (left), shape index(middle) and curvedness(right).

Two-dimensional fingerprint plots (Figure 8) obtained from Hirshfeld surface analysis may also be useful to shed light on the supramolecular interactions, which appear as distinct spikes in this plot. Complementary regions are observable in the two-dimensional fingerprint plots where one molecule act as donor ($d_e > d_i$) and the other as an acceptor ($d_e < d_i$). In the fingerprint plot of complex **1**, the most dominant interactions are found for $N\cdots H/H\cdots N$ contacts, which contribute to 26.0% of the total Hirshfeld surface. However in complex **2**, $N\cdots H/H\cdots N$ interactions contribute only 5.9%. The proportions of $C\cdots H/H\cdots C$ interactions comprise 11.7 and 11.8% of the Hirshfeld surfaces for each molecule of complexes **1** and **2** respectively. On the other hand very less contribution of interactions is coming from $O\cdots H$ contacts i.e. 5.5% and 9% in complexes **1** and **2** respectively.

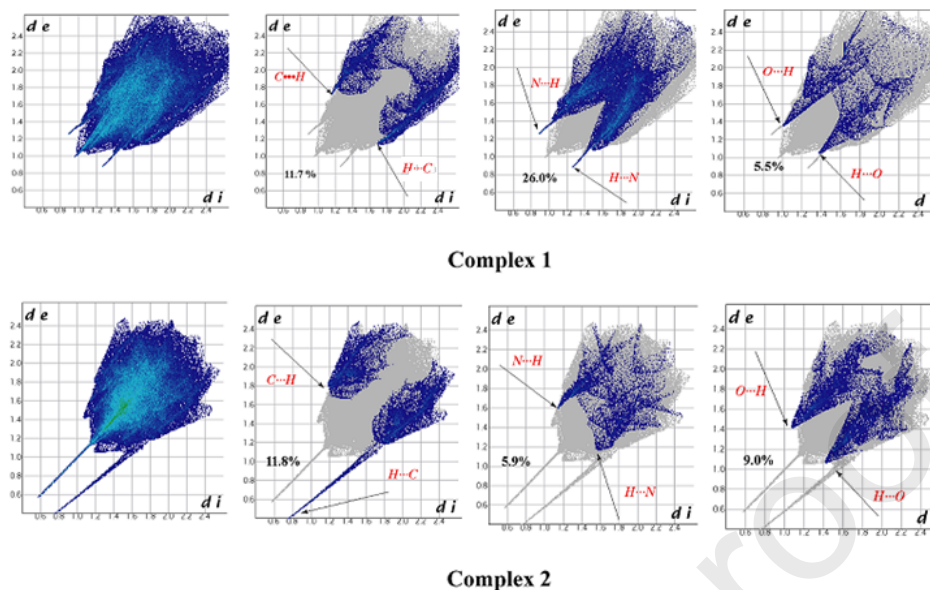


Figure 8: Fingerprint plot: Full (a), resolved into H...C/C...H (b), H...N/N...H (c) and H...O/O...H (d) contacts contributed to the total Hirshfeld Surface.

At this stage it is relevant to construct a histogram of relative areas as discussed above. Thus with the help of the histogram one may minutely differentiate the magnitude of the supramolecular interactions between two complexes. Hence the percentage contributions of significant atom-type/atom-type contacts to the Hirshfeld surfaces have been elucidated in Figure 9 in the form of histograms, which clearly indicate that in the solid state structure, supramolecular interactions involving N...H hydrogen bonding are highly significant in complex 1.

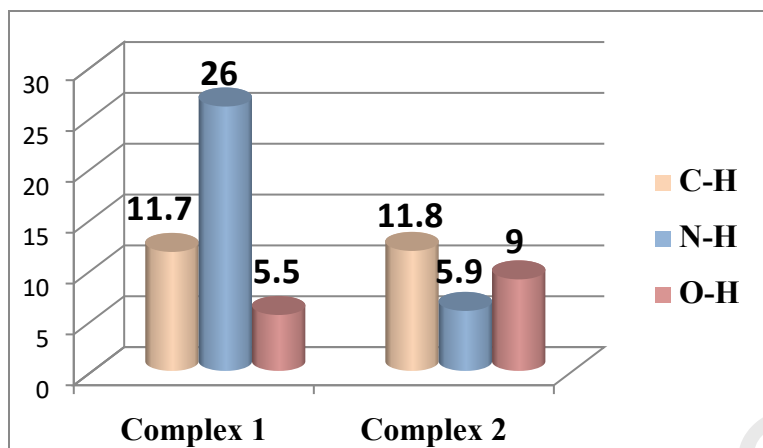


Figure 9: Percentage contributions to the Hirshfeld surface area for significant close intermolecular contacts in complexes

3.6. Spectral and magnetic details

The IR spectra of both complexes exhibit moderately strong sharp peaks in the range of 3195-3210 cm^{-1} which may be assigned as N-H stretching vibrations [60]. In the IR spectrum of complex **1**, a bifurcated sharp band in the range of 2035-2056 cm^{-1} corresponds to the presence of azide groups. On the other hand, a sharp peak at 2051 cm^{-1} in the IR spectrum of complex **2** also supports the presence of azide groups [2]. The presence of carboxylato ligand has been confirmed by the appearance of a strong and sharp peak (at 1562 cm^{-1} in **1** and 1577 cm^{-1} in **2**) along with a shoulder (at 1480 cm^{-1} in **1** and 1485 cm^{-1} in **2**) in the IR spectrum of each complex [61-63]. The bands corresponding to alkyl C-H stretching vibrations occur in the range of 2960-2848 cm^{-1} . IR spectra of complexes **1** and **2** have been given in Figures S2 and S3 (SI) respectively.

The electronic spectra (800-200 nm) of complexes **1** and **2** have been depicted in Figures S4 and S5 (SI) respectively. Most often low spin cobalt(III) complexes show two broad absorption bands at low energy region due to ${}^1A_{1g} \rightarrow {}^1T_{1g}$ and ${}^1A_{1g} \rightarrow {}^1T_{2g}$ transitions which are

spin allowed [64]. The broad absorption band (at 620 nm for **1** and 706 nm for **2**) in the electronic spectra of complexes **1** and **2** may be assigned as one of the two expected (mentioned above) transitions. The other spin allowed transition gets obscured due to the large intensity of LMCT bands [65]. The intense absorption bands of the complexes, at around 355 nm have been assigned as charge transfer transitions from the coordinated ligands to the cobalt(III) centers (LMCT) [66]. High energy absorption bands at 245 nm in complex **1** and 255 nm in complex **2** may be assigned to intra ligand $\pi - \pi^*$ transition [67].

The effective magnetic moment of complex **1** has been measured to about 5.17 B.M. at room temperature, and this is slightly higher from that expected for three unpaired electrons present in the high spin (HS) cobalt(II) system. Cobalt(III) is essentially low spin with t_{2g}^6 electronic configuration and therefore do not contribute any spin magnetic moment. From the magnetic point of view, therefore, this dinuclear mixed valence cobalt(III/II) complex may be considered as a cobalt(II) monomer with $^4T_{1g}$ ground state term. Therefore, it shows high magnitude of orbital contribution to the total magnetic moment in its ground state, which is the reason for deviation from spin only magnetic moment value. Recently a similar kind of dinuclear mixed valence cobalt(III/II) complex has been synthesized by our group [68] and its magnetic nature is also explored. It suggests that such kind of complex belongs to localized class-I mixed valence system with isolated $S = 3/2$ ion and there may be no significant spin delocalisation between cobalt(II) and cobalt(III) center. On the other hand, complex **2** is found to be diamagnetic, as expected for low spin cobalt(III) complexes [69-76].

3.7. Molar conductivity

The molar conductivity values of complexes **1** and **2** in nitrobenzene were found as 0.03 and 0.002 $\text{Scm}^2\text{mol}^{-1}$ respectively, which were in good agreement with values expected for a

non-electrolyte. This suggested that the coordinated azide and acetate did not ionize in nitrobenzene.

3.8. Kinetics study and explanation of the turnover numbers

The saturation rate dependency on the concentration of the substrate can be calculated using Michaelis-Menten model. According to the Michaelis-Menten equation

$$V = \frac{V_{max} [S]}{K_M + [S]} \dots (1)$$

Where, V = initial rate; $[S]$ = concentration of the substrates; K_M = Michaelis-Menten constant for complex and V_{max} = maximum initial rate achieved for a particular concentration of the complex in the presence of a large amount of the substrate.

On the other hand, rearrangement of Michaelis-Menten equation produces three new equations i.e. Lineweaver-Burk equation (eq. 2), Hanes equation (eq. 3) and Eadie-Hofstee equation (eq. 4).

$$\frac{1}{V} = \frac{K_M}{V_{max}} \frac{1}{[S]} + \frac{1}{V_{max}} \dots (2)$$

$$\frac{[S]}{V} = \frac{[S]}{V_{max}} + \frac{K_M}{V_{max}} \dots (3)$$

$$V = V_{max} - K_M \frac{V}{[S]} \dots (4)$$

Variety of kinetic parameters, including turnover number (k_{cat}) and specificity constant (k_{cat}/K_M) for phenoxazinone synthase mimicking activity of synthesized complexes can be analysed using all these equations. Kinetic parameters like V_{max} and K_M have been calculated by the analysis of entire experimental data. Figure 10 depicts the time dependent spectral change for the period of 2 h after the addition of 2-aminophenol to the acetonitrile medium of complex 1. The turnover number value (k_{cat}) has been calculated by dividing the V_{max} by the concentration

of the catalyst (complex) used. Figure 11 represents the Michaelis-Menten plot, Lineweaver-Burk plot, Hanes plot and Eadie-Hofstee plot of complex **2** for catalytic oxidation of 2-AP, respectively. Such kind of plots for complex **1** has been provided in Figures S6-S7 (SI). Both the complexes show a reactivity pattern very similar to each other. In order to calculate kinetic parameters more accurately, several enzyme kinetic plots have been used. Similar kind of kinetic parameters have been obtained in all cases which indicate the accuracy of the experimental results. The k_{cat} values (Table 6) suggest that both the complexes act as effective catalyst for the conversion of 2-aminophenol to 2-aminophenoxazine-3-one. Kinetic parameters of some of the reported cobalt complexes for phenoxazinone synthase like activity have been depicted in [Table 6](#). Control experiments were performed using 10^{-4} M $\text{Co}(\text{OAc})_2 \cdot 4\text{H}_2\text{O}$ and 10^{-2} M of 2-AP, where no drastic change has been observed in absorption intensity even after several hours.

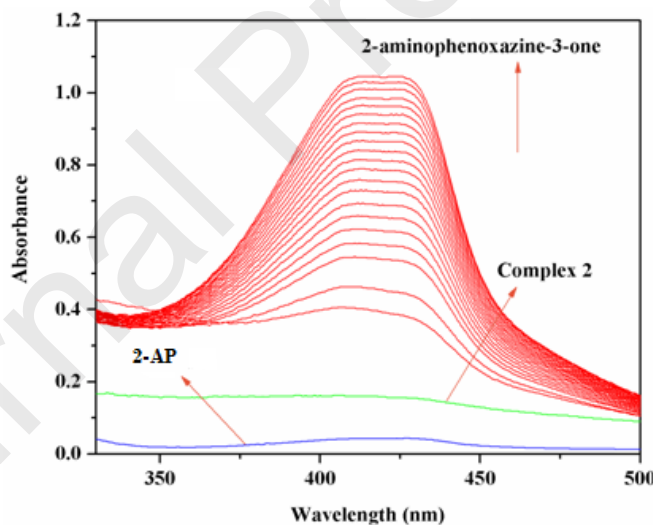


Figure 10: Time resolved UV-Vis spectral profile indicating the increment of 2-aminophenoxazine-3-one peak at ~ 433 nm upon addition of 10^{-2} M 2-aminophenol to the 10^{-4} M of complex **2** in acetonitrile medium at room temperature (298 K).

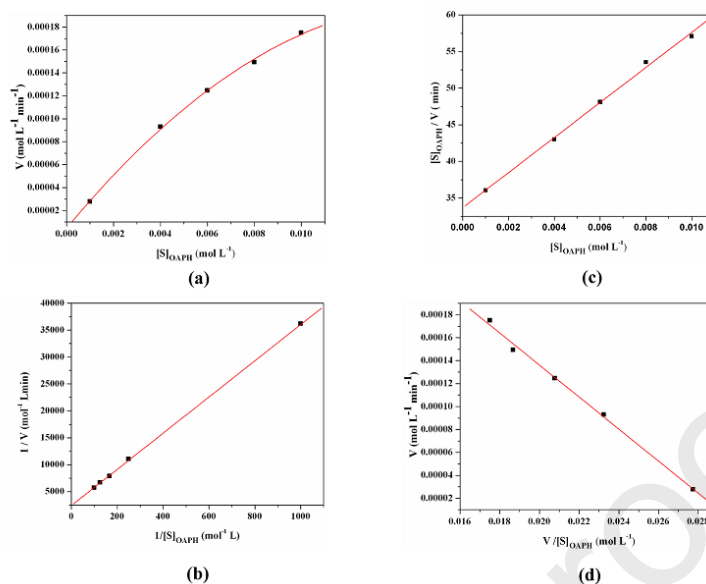


Figure 11: Michaelis–Menten plot (a), Lineweaver–Burk plot (b), Hanes plot (c) and Eadie–Hofstee plot (d) for catalytic oxidation of 2-AP in acetonitrile medium at room temperature (298 K) using complex **1** as catalyst.

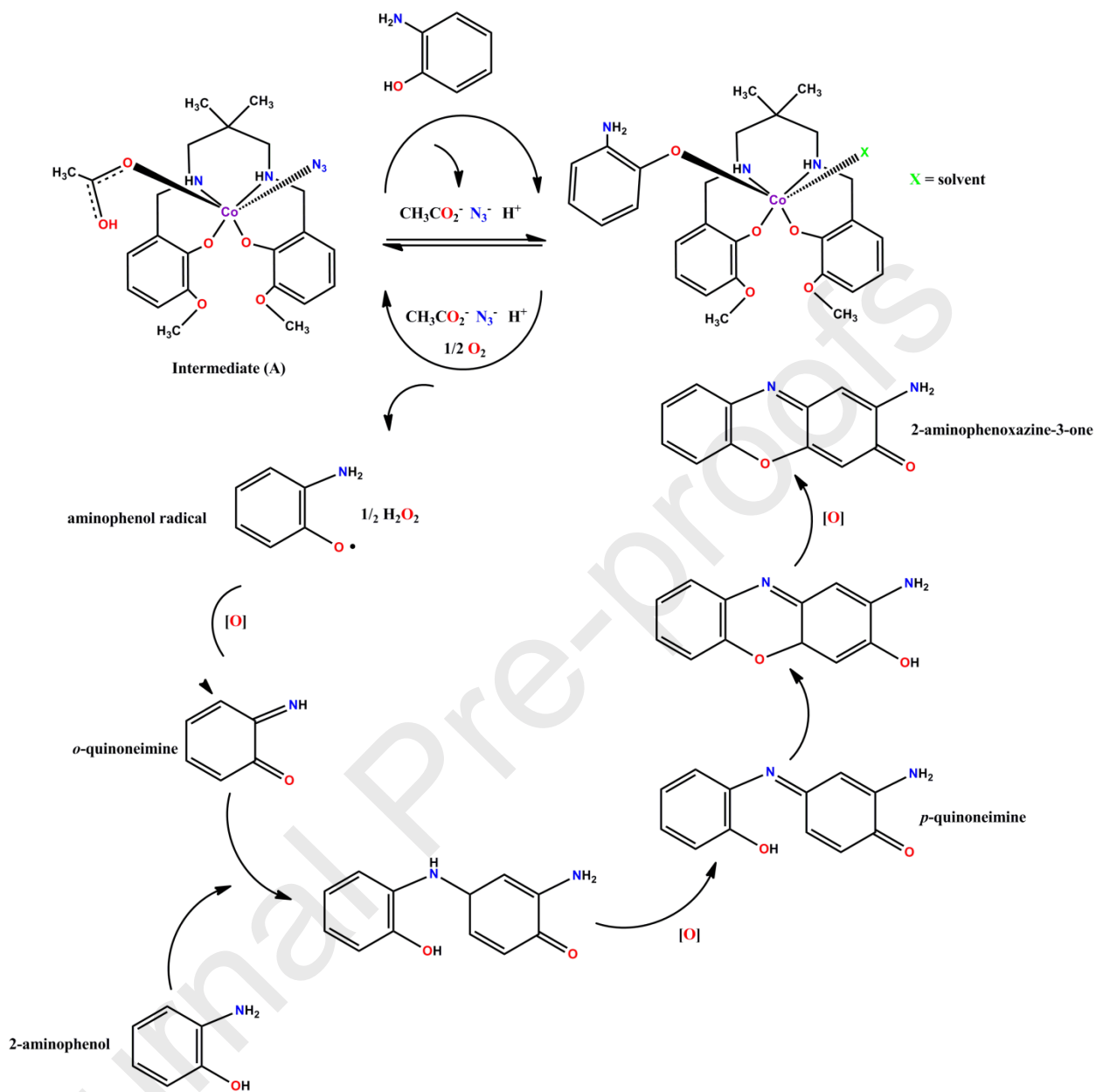
Table 6: Kinetic parameters for the 2-AP mimicking activity of complexes **1** and **2** in acetonitrile.

Complex	V _{max} (mol L ⁻¹ min ⁻¹)	K _M (mol L ⁻¹)	K _{Cat} (h ⁻¹)
1	4.17 x10 ⁻⁴	14.02x10 ⁻³	250.21
2	8.23 x10 ⁻⁴	2.32x10 ⁻²	493.73

3.8. Mechanism of catalysis

The experimental results are in nice agreement with the moderate catalytic activity of both complexes to mimic phenoxazinone synthase. At the beginning, both complexes liberate the metal centers from the outer O₄ compartments (Cobalt(II) in **1** and Na in **2**) to produce the intermediate species (say A), as concluded from the ESI mass spectra of the complexes and the mass spectra of the complexes with 2-aminophenol in 1:50 ratio (Figures 12, 13, S8 and S9, see

below). 2-aminophenol then forms adduct with this intermediate species (A) liberating monodentate azide and acetate, and this adduct, in turn, produces 2-aminophenol radical by the reaction with molecular dioxygen and thereby regenerates the intermediate (A). The 2-aminophenol radical may generate *ortho*-benzoquinone monoamine, which can then easily be converted to 2-aminophenoxazine-3-one by the reaction with dioxygen and 2-aminophenol [77]. Scheme 3 highlights the probable mechanism for catalytic conversion of 2-aminophenol to 2-aminophenoxazine-3-one by the individual complexes **1** and **2**.



Scheme 3: Probable mechanistic pathway showing the formation of 2-aminophenoxazine-3-one by the prepared cobalt complexes, **1** and **2**.

From the detailed kinetic analysis, it is evident that complex **2** acts as more efficient catalyst for the aerobic oxidation of 2-aminophenol, while complex **1** is relatively less reactive. This may be correlated with the lability of the metal ion present in the outer O_4 compartment.

Since cobalt(II) is more crystal field stabilized than sodium ion (CFSE = 0 for Na ion), sodium ion eliminates out from the outer compartment at much faster rate compared to cobalt(II), leading to higher k_{cat} value for complex **2**. Synonymous plausible catalytic cycles of this phenoxazinone synthase mimicking catalytic activity have been also projected by other groups over the past years (see below).

Table 7: Turn over numbers for the oxidation of 2-AP to 2-aminophenoxazine-3-one catalyzed by various reported cobalt complexes.

Complexes	TON (h ⁻¹)	Solvent	Reference
$[Co^{II}(L^1)Cl_2]$	4.10	Methanol	78
$[Co^{II}(L^2)(NCS)_2]$	7.38	Methanol	
$[Co^{II}(L^2)Cl(H_2O)]Cl \cdot H_2O$	13.68	Methanol	
$[Co^{II}(L^3)(CH_3CN)](ClO_4)_2$	3.36	Methanol	79
$[Co^{II}(L^4)(H_2O)](ClO_4)_2$	6.37	Methanol	
$[Co^{II}(L^5)(H_2O)](ClO_4)_2$	8.28	Methanol	
$[Co^{III}_2(L^6)_2(\mu-O_2)](ClO_4)_4$	23.04	Methanol	
$[Co^{III}_2(L^7)_2(\mu-O_2)](ClO_4)_4 \cdot 2CH_3CN$	30.09	Methanol	
$[Co^{III}(L^8)(L^9)(N_3)]$	8.32	Methanol	80
$[Co^{III}(L^{10})(L^{11})_2]ClO_4 \cdot MeOH \cdot H_2O$	11.48	Methanol	81
$[Co^{III}(L^{10})(L^{12})_2Na(ClO_4)_2] \cdot 0.5H_2O$	27.90	Methanol	
$[Co^{III}_2(L^{13})_2(\mu-L^{14})_2Cl_2]Cl_2 \cdot 2H_2O$	13.75	Methanol	82
$[Co^{III}(HL^{15})_2][Co^{II}(NCS)_4]NCS$	8.37	Methanol	

$[Co^{III}(L^{15})_2][Co^{II}(NCO)_4]$	26.1	Methanol	83
$[Co^{III}(L^{15})(NCS)_2] \cdot 0.5H_2O$	48.6	Methanol	
$[Co^{III}(L^{15})(N_3)_2] \cdot 0.5CH_3CN$	54	Methanol	
$[Co^{III}(L^{16})(N_3)_3]$	20.37	Methanol	84
$[Co^{III}(L^{17})(N_3)_3]$	33.26	Methanol	
$[Co^{III}(L^{18})_2(L^{19})_2]Cl \cdot 8H_2O$	30.60	Methanol	85
$[Co^{III}(L^{20})(L^{21})(N_3)]$	72.12	Acetonitrile	86
$[Co^{III}(L^{22})(L^{23})(N_3)]$	77.52	Acetonitrile	
$[Co^{III}_2Co^{II}(L^{24})_2(\mu^2-C_6H_5CO_2)_2(C_6H_5CO_2^-)_2] \cdot (CH_3CN)_2$	153.60	Acetonitrile	18
$[Co^{III}(L^{20})(L^{25})(N_3)]$	247.2	Acetonitrile	87
$[Co^{III}(L^{20})(L^{25})(NCS)]$	257.4	Acetonitrile	
$[Co^{III}(L^{26})(L^{27})(N_3)]$	351.68	Methanol + Acetonitrile	88
$[Co^{III}(L^{27})(L^{28})(N_3)]$	355.28	Methanol + Acetonitrile	
$[Co^{III}(L^{29})(L^{30})(N_3)]$	166.64	Acetonitrile	89
$[Co^{III}(L^{31})(L^{32})(NCS)]$	626.40	Acetonitrile	
$[Co^{III}(L^{33})_2](ClO_4)_3$	5120	Acetonitrile	69
$[(N_3)Co^{III}L^{34}(\mu-C_6H_5COO)Co^{II}(N_3)] \cdot CH_3OH$	153.90	Methanol	34
$[(N_3)Co^{III}L(\mu-OAc)Co^{II}(N_3)]$	250.21	Acetonitrile	

$(\mu-N_3)_2[(N_3)Co^{III}(L)Na(OMe)]_2 \cdot CH_3OH$	493.73	Acetonitrile	This Work
---	--------	--------------	------------------

$L^1 = N,N'$ -bis(6-methylpyridin-2-ylmethylene)-2,2-dimethylpropane-1,3-diamine; $L^2 = N,N'$ -bis(pyridin-2-ylmethylene)-2,2-dimethylpropane-1,3-diamine; $L^3 = 1 : 2$ condensation product of diethylenetriamine and 2-pyridinecarboxaldehyde; $L^4 = 1 : 2$ condensation product of 3,3'-bisaminopropylamine and 6-methyl-2-pyridinecarboxaldehyde; $L^5 = 1 : 2$ condensation product of 3,3'-diamino-*N*-methyldipropylamine and 6-methyl-2-pyridinecarboxaldehyde; $L^6 = 1 : 2$ condensation product of 3,3'-bisaminopropylamine and 2-acetylpyridine; $L^7 = 1 : 2$ condensation product of 3,3'-bisaminopropylamine and 2-pyridinecarboxaldehyde; $HL^8 = 1$ -((2-(diethylamino)ethylimino)methyl)naphthalene-2-ol; $HL^9 =$ acetylacetone, $H_2L^{10} = N,N'$ -bis(3-methoxysalicylaldehyde)cyclohexane-1,2-diamine); $L^{11} = 4$ -aminopyridine; $L^{12} = 1$ -methylimidazole; $L^{13} = 2$ -aminomethylpyridine; $L^{14} = 2$ -iminomethylpyridine anion; $HL^{15} =$ condensation product of *N,N'*-dimethyldipropylenetriamine and *o*-vanillin; $L^{16} =$ bis(2-pyridylmethyl)amine; $L^{17} = (2$ -pyridylmethyl)(2-pyridylethyl)amine; $H_2L^{18} = 3,5,6$ -tribromo-4-pyridiniumcatechol; $L^{19} =$ pyridine; $HL^{20} = 1$ -benzoylacetone; $HL^{21} = 1$ ((2-(diethylamino)ethylimino)methyl)naphthalen-2-ol; $HL^{22} = 2$ -acetyl-1-naphthol; $HL^{23} = 2$ ((2(2-hydroxyethylamino)ethylimino)methyl)-6-ethoxyphenol; $H_2L^{24} = N$ -(2-hydroxyethyl)-3-methoxysalicylaldehyde; $HL^{25} = 2$ -(3-(dimethylamino)propylimino)methyl)-6-ethoxyphenol; $H_2L^{26} = 2$ ((3-(dimethylamino)propylimino)methyl)-6-ethoxyphenol; $HL^{27} = 5$ -(2-pyridyl)tetrazole; $H_2L^{28} = 2$ ((3-(methylamino)propylimino)methyl)-6-methoxyphenol; $HL^{29} = 2$ ((2(piperidin-1-yl)ethylimino) methyl)-6-ethoxyphenol; $HL^{30} = 1$ -acetyl-2-naphthol; $HL^{31} = 2$ -(3(dimethylamino)propylimino)methyl)-6-methoxyphenol; $HL^{32} = 2,4$ -pentanedione; $L^{33} =$

condensation product of 1,3-propanediamine and 2-benzoylpyridine. $H_2L^{3+} = (1,3\text{-propanediyl})\text{bis}(\text{iminomethylene})\text{bis}(6\text{-methoxyphenol})]$

On the basis of k_{cat} values, comparison can be made between the catalytic efficiency of these synthesized cobalt complexes with other cobalt based model complexes showing phenoxazinone synthase mimicking activity assembled in Table 7. Both these complexes are behaving as more efficient catalyst compared to many other cobalt(III) and cobalt (II) complexes [18,77-86]. However there are some cobalt(III) complexes reported in literature to show more catalytic activity than present complexes [69,87-88]. Hence these complexes can be considered as moderate catalysts showing phenoxazinone synthase mimicking activity.

3.9. ESI mass spectral analysis

To get better understanding of the nature of catalyst-substrate intermediate of phenoxazinone-synthase like activity in acetonitrile medium and support the idea behind the proposed catalytic cycle, the ESI mass spectral analysis (ESI-MS positive) of both complexes have been recorded with and without the presence of substrate (2-aminophenol for phenoxazinone synthase mimicking activity).

Complex 1: The ESI-MS spectrum of the complex in acetonitrile shows a peak (Figure 12) at m/z 530.11 (calc. 529.19) which may be assigned as the ionic fragment, $[(AcO)\text{-Co}^{III}\text{-L-Li}]^+\text{-CH}_3\text{OH}$. Another peak at $m/z = 450.62$ (calc. 449.14) of high intensity is due to the fragment, $[\text{Co}^{III}\text{-L}]^+\text{-H}_2\text{O}$.

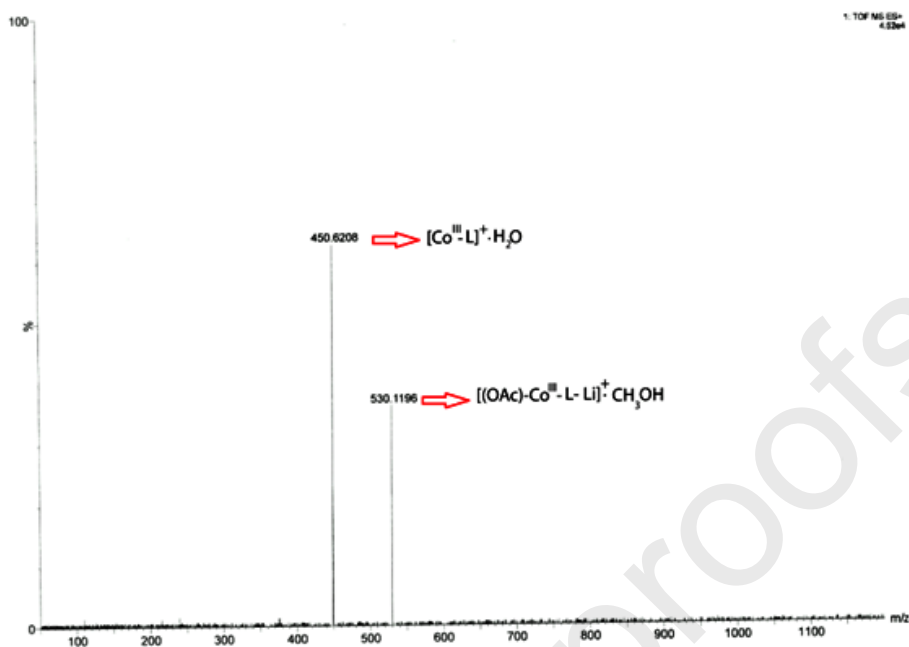


Figure 12: ESI-MS positive spectrum of complex **1** in acetonitrile medium at room temperature.

Complex 2: The ESI-MS positive spectrum of the complex in acetonitrile has been depicted in Figure S8 (SI). A sharp peak is noticed at $m/z = 454.11$ (calc. 454.62) which may be assigned to the presence of a ionic fragment, $[H_2L-CH_3CN-K]^+$.

1:50 mixture of complexes 1 and 2 with 2-AP: In addition ESI-MS positive spectrum of 1:50 mixture of both complexes with 2-aminophenol have been recorded separately after 5 min of mixing in acetonitrile. The most prominent investigation from the mass spectral study is the appearance of peaks related to substrate-catalyst intermediate species, formed after adding 2-AP to the acetonitrile solution of each complex.

The mixture of complex **1** and 2-AP in a molar ratio of 1:50 in acetonitrile resulted a peak at $m/z = 577.07$ (calc. 577.21) in the mass spectrum. This indicates the formation of the substrate-catalyst intermediate species, $[Co^{III}-L-(2-aminophenolate)-CH_3OH-Li]^+$. This peak

verifies that the catalytic cycle proceeds through a stable substrate-catalyst intermediate formation. ESI-MS positive spectra of 1:50 mixture of complex **1** with 2-aminophenol have been demonstrated in Figure 13. Two other sharp peaks appear at $m/z = 454.12$ (cal. 454.62) and 375.23 (calc. 375.48) correspond to $[H_2L-CH_3CN-K]^+$ and $[H_2L-H]^+$ respectively. Moreover, in presence of 2-aminophenol a peak appears at $m/z = 215.08$ (calc. 215.07) which supports the formation of protonated 2-aminophenoxazine-3-one, $[C_{12}H_{11}N_2O_2]^+$ and confirms the phenoxazinone synthase mimicking activity of the complex **1**.

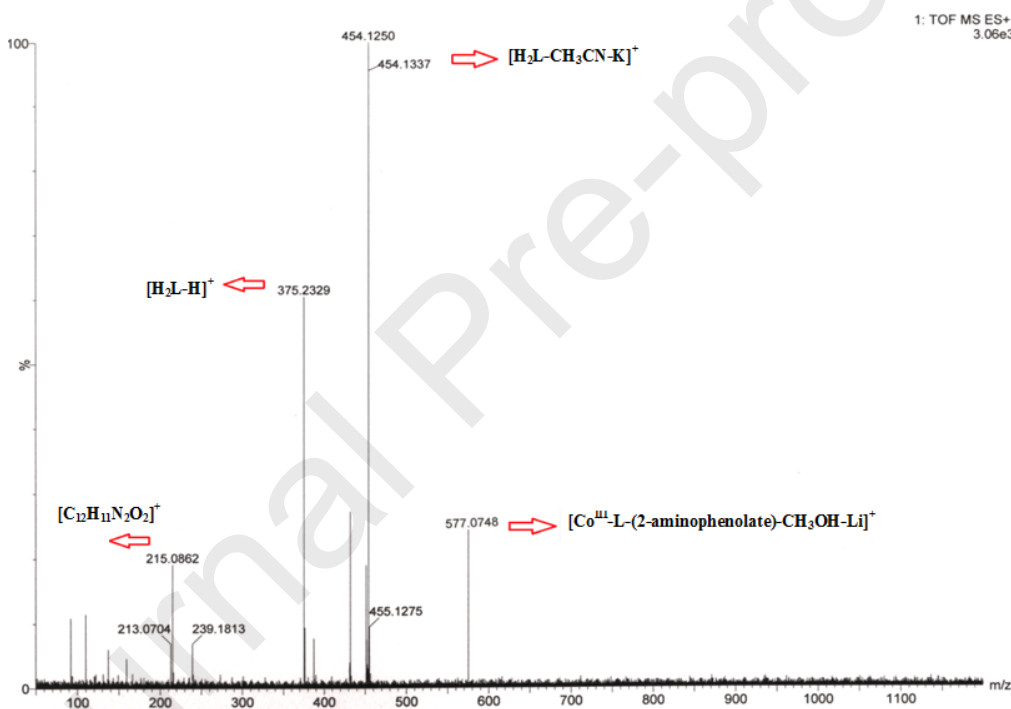


Figure 13: ESI-MS positive spectrum of 1:50 mixture of complex **1** and 2-aminophenol in acetonitrile medium at room temperature.

Very similar peaks are found in the mass spectrum of the 1:50 mixture of complex **2** and 2-aminophenol as that in complex **1**. Sharp peaks appearing at 375.22 (calc.375.48) and 454.11 (calc.454.62) suggest the formation of protonated reduced Schiff base ligand species, $[H_2L-H]^+$

and $[H_2L-CH_3CN-K]^+$ respectively. Another sharp peak of maximum intensity at $m/z = 432.13$ (calc.431.39) corresponds to the presence of an ionic fragment, $[Co^{III}-L]^+$. The peak at $m/z = 635.04$ (calc.636.17) may indicate the formation of a substrate-catalyst adduct, $[Co^{III}-L-(2-aminophenolate)-CH_3CN-K]^+ \cdot H_2O$. In addition a characteristic peak at $m/z = 215.18$ (calc. 215.07) is also noticed which corresponds to protonated 2-aminophenoxazine-3-one, $[C_{12}H_{11}N_2O_2]^+$. Thus the proposed mechanistic pathway has been justified by the mass spectral analysis. ESI-MS positive spectrum of 1:50 mixture of complex **2** with 2-aminophenol has been demonstrated in Figure S9 (SI).

4. Conclusion

The present study demonstrates the synthetic strategy of a dinuclear mixed valence cobalt(III)/cobalt(II) complex (**1**) and a tetranuclear cobalt(III)/sodium complex (**2**), starting from the same substrate and appropriate reagents. The formation of complexes **1** and **2** is jointly controlled by the amount of cobalt(II) precursors present in the reaction mixture and the pH of the medium. In addition, both complexes are found to act as functional models of phenoxazinone synthase. Complex **2** is showing higher catalytic ability compared to complex **1** and this may be correlated with the lability of the metal ion present in the outer O_4 compartment, cobalt(II) in complex **1** and sodium in complex **2**. Since cobalt(II) is more crystal field stabilized compared to sodium ion (CFSE is 0 for sodium), sodium ion eliminates out from the outer O_4 compartment at much faster rate compared to cobalt(II), and this is reflected in their k_{cat} values; 250.21 and 493.73 h^{-1} for **1** and **2** respectively.

Acknowledgments

A. B. thanks the UGC, India, for awarding a Junior Research Fellowship. S. C wishes to thank the RUSA 2.0 program of the Government of India, operating at Jadavpur University under which they each received “Research Support to Faculty Members” for Research Thrust Areas “Research in Advance Materials”; Sanction Ref. no. R-11/755/19 dated 27.06.2019.

Appendix A. Supplementary data

Supplementary information (SI) available: Hirshfeld Surface Analysis, Tables from S1-S3 and Figures from S1-S9. CCDC 2011893-2011894 contain the supplementary crystallographic data for complexes **1** and **2** respectively. This data can be obtained free of charge via <http://www.ccdc.cam.ac.uk/conts/retrieving.html>, or from the Cambridge Crystallographic Data Centre, 12 Union Road, Cambridge CB2 1EZ, UK; fax: (+44) 1223-336-033; or e-mail: deposit@ccdc.cam.ac.uk.

References

- [1] D. M. D’Alessandro, F. R. Keene, *Chem. Rev.* 106 (2006) 2270.
- [2] A. Banerjee, S. Banerjee, C. G. García, S. Benmansour, S. Chattopadhyay, *ACS Omega* 4 (2019) 20634.
- [3] S. K. Dutta, J. Ensling, R. Werner, U. Flörke, W. Haase, P. Güttlich, K. Nag, *Angew. Chem., Int. Ed. Engl.* 36 (1997) 834.
- [4] S. Druke, P. Chaudhuri, K. Pohl, K. Wieghardt, X.-Q. Ding, E. Bill, A. Sawaryn, A. X. Trautwein, H. Winkler and S. J. Gurman, *J. Chem. Soc., Chem. Commun.* (1989) 59.
- [5] L. Suchow, *J. Chem. Educ.* 53, 9 (1976) 560.

- [6] D. R. Rosseinsky, R. J. Mortimer, *Adv. Mater.* 13 (2017) 83.
- [7] M. B. Coban, E. Gungor, H. Kara, U. Baisch, Y. Acar, *J. Mol. Struct.* 1154 (2018) 579.
- [8] L.-L. Hu, Z.-Q. Jia, J. Tao, R.-B. Huang, L.-S. Zhen, *Dalton Trans.* (2008) 6113.
- [9] S. Majumder, S. Mondal, P. Lemoine, S. Mohanta, *Dalton Trans.* 42 (2013) 4561.
- [10] L. Mandal, S. Mohanta, *Dalton Trans.* 43 (2014) 15737.
- [11] R. Modak, Y. Sikdar, S. Mandal, S. Goswami, *Inorg. Chem. Commun.* 37 (2013) 193.
- [12] K. Ghosh, K. Harms, A. Bauzá, A. Frontera, S. Chattopadhyay, *CrystEngComm* 20 (2018) 7281.
- [13] J. Luo, N. P. Rathand, L. M. Mirica, *Inorg. Chem.* 50 (2011) 6152.
- [14] W. Zhu, S. Zhang, C. Cui, F. Bi, H. Ke, G. Xie and Sanping Chen, *Inorg. Chem. Commun.* 46 (2014) 315.
- [15] S. Chattopadhyay, G. Bocelli, A. Musatti, A. Ghosh, *Inorg. Chem. Commun.* 9 (2006) 1053.
- [16] A. Banerjee, S. Chattopadhyay, *Polyhedron* 159 (2019) 1.
- [17] A. Hazari, L. K. Das, R. M. Kadam, A. Bauzá, A. Frontera, A. Ghosh, *Dalton Trans.* 44 (2015) 3862.
- [18] A. Hazari, A. Das, P. Mahapatra, A. Ghosh, *Polyhedron* 134 (2017) 99.
- [19] F. Zamora, H. Witkowski, E. Freisinger, J. Müller, B. Thormann, A. Albinati, B. Lippert, *J. Chem. Soc., Dalton Trans.* (1999) 175.

- [20] J. Xue, X. Hua, L. Yang, W. Li, Y. Xu, G. Zhao, G. Zhang, L. Liu, K. Liu, J. Chen, J. Wu, *J. Mol. Struct.* 1059 (2014) 108.
- [21] I. Koehne, R. Herbst-Irmer and D. Stalke, *Eur. J. Inorg. Chem.* (2017) 3322.
- [22] K. Reuter, S. S. Rudel, M. R. Buchner, F. Kraus, C. von Hänisch, *Chem. – Eur. J.* 23 (2017) 9607.
- [23] G. Arom^ì, A. R. Bell, M. Helliwell, J. Raftery, S. J. Teat, G. A. Timco, O. Roubeau, R. E. P. Winpenny, *Chem. – Eur. J.* 9 (2003) 3024.
- [24] D. Cunningham, P. McArdle, M. Mitchell, N. N^íchonchubhair, M. ^ÓGara, F. Franceschi, C. Floriani, *Inorg. Chem.* 39 (2000) 1639.
- [25] N. Mahlooji, M. Behzad, H. A. Rudbari, G. Bruno, B. Ghanbari, *Inorg. Chim. Acta* 445 (2016) 124.
- [26] E. E. Moushi, C. Lampropoulos, W. Wernsdorfer, V. Nastopoulos, G. Christou, A. J. Tasiopoulos, *Inorg. Chem.* 46 (2007) 3795.
- [27] S. Mandal, N. Hari, S. Mondal, S. Mohanta, *Inorg. Chim. Acta* 483 (2018) 527.
- [28] A. Das, S. Goswami, R. Sen, A. Ghosh, *Inorg. Chem.* 58 (2019) 5787.
- [29] S. Maity, A. Mondal, S. Konar, A. Ghosh, *Dalton Trans.* 48 (2019) 15170.
- [30] K. Ghosh, K. Harms, A. Bauzá, A. Frontera, S. Chattopadhyay, *Dalton Trans.* 47 (2018) 331.
- [31] A. Banerjee, A. Frontera, S. Chattopadhyay, *Dalton Trans.* 48 (2019) 11433.

- [32] M. Das, S. Chatterjee, S. Chattopadhyay, *Inorg. Chem. Commun.* 14 (2011) 1337.
- [33] M. Karmakar, T. Basak, S. Chattopadhyay, *New J. Chem.* 43 (2019) 4432.
- [34] A. Banerjee, S. Chattopadhyay, *Polyhedron* 177 (2020) 114290.
- [35] M. Karmakar, S. Roy, S. Chattopadhyay, *New J. Chem.* 43 (2019) 10093.
- [36] G. M. Sheldrick, *Acta Crystallogr. Sect. C: Struct. Chem.* 71 (2015) 3.
- [37] G.M. Sheldrick, *SADABS: Software for Empirical Absorption Correction*, University of Gottingen, Institute fur Anorganische Chemieder Universitat, Gottingen, Germany, 1999–2003.
- [38] S. Roy, T. Basak, S. Khan, M. G. B. Drew, A. Bauza, A. Frontera, S. Chattopadhyay, *ChemistrySelect* 2 (2017) 9336.
- [39] A. Bhattacharyya, S. Roy, J. Chakraborty, S. Chattopadhyay, *Polyhedron* 112 (2016) 109.
- [40] S. Roy, M. G. B. Drew, S. Chattopadhyay, *Polyhedron* 150 (2018) 28.
- [41] M. Sarwar, A.M. Madalan, C. Maxim, M. Andruh, *Rev. Roum. Chem.* 57 (2012) 687.
- [42] J.-P. Costes, F. Dahan, J. Garcia-Tojal, *Chem. Eur. J.* 8, (2002), 5430.
- [43] P. Costes, F. Dahan, W. Wernsdorfer. *Inorg. Chem.* 45, (2006), 5.
- [44] P. K. Bhaumik, A. Banerjee, T. Dutta, S. Chatterjee, A. Frontera, S. Chattopadhyay, *CrystEngComm*, 2020, 22, 2970.
- [45] K. Ghosh, K.Harms, A. Bauzá, A. Frontera, S. Chattopadhyay, *Dalton Trans.* 47 (2018) 331.
- [46] S. MirDYa, S. Banerjee, S. Chattopadhyay, *CrystEngComm* 22, (2020), 237.

- [47] S. Mirdya, M. G. B. Drew, A. K. Chandra, A. Banerjee, A. Frontera, S. Chattopadhyay, S. Mirdya, *Polyhedron* 179 (2020) 114374.
- [48] S. Mirdya, S. Roy, S. Chatterjee, A. Bauza, A. Frontera, S. Chattopadhyay, *Cryst. Growth Des.* 19 (2019) 5869.
- [49] S. Mirdya, T. Basak, S. Chattopadhyay, *Polyhedron* 170 (2019) 253.
- [50] S. Chattopadhyay, A. Frontera, M. Karmakar, *CrystEngCom* doi.org/10.1039/D0CE01105C
- [51] N. E. Brese, M. O'Keeffe, *Acta Cryst.* B47 (1991) 192.
- [52] I. D. Brown, D. Altermatt, *Acta Cryst.* B41 (1985) 244.
- [53] M. O'Keeffe, N. E. Brese, *J. Am. Chem. Soc.* 113 (1991) 3226.
- [54] H. H. Thorp, *Inorg. Chem.* 31 (1992) 1585.
- [55] G. J. Palenik, *Inorg. Chem.* 36 (1997) 122.
- [56] R. M. Wood, G. J. Palenik, *Inorg. Chem.* 37 (1998) 4149.
- [57] N. M. Boyle, A. C. Coleman, C. Long, K. L. Ronayne, W. R. Browne, B. L. Feringa, M. T. Pryce, *Inorg. Chem.* 49 (2010) 10214.
- [58] K. C. Mondal, P. P. Samuel, H. W. Roesky, E. Carl, R. Herbst-Irmer, D. Stalke, B. Schwederski, W. Kaim, L. Ungur, L. F. Chibotaru, M. Hermann, G. Frenkin, *J. Am. Chem. Soc.* 136 (2014) 1770.
- [59] D. Cremer, J. A. Pople, *J. Am. Chem. Soc.* 97 (1975) 1354.

- [60] C. T. Yang, B. Moubaraki, K. S. Murray, J. D. Ranford, J. J. Vittal, *Inorg. Chem.* 40 (2001) 5934.
- [61] A. K. Sharma, F. Lloret, R. Mukherjee, *Inorg. Chem.* 52 (2013) 4825.
- [62] B. Cristóvão, B. Mirosław, J. Kłak, M. Rams, *Polyhedron* 85 (2015) 697.
- [63] A. K. Sharma, F. Lloret and R. Mukherjee, *Inorg. Chem.* 52 (2013) 4825.
- [64] S. Chattopadhyay, M. G. B. Drew, A. Ghosh, *Eur. J. Inorg. Chem.* (2008) 1693.
- [65] A. Kufelnicki, S. V. Tomy, Y. S. Moroz, M. Haukka, J. J. Rosińska, I. O. Fritsky, *Polyhedron* 33 (2012) 410.
- [66] M. Galini, M. Salehi, M. Kubicki, A. Amiri, A. Khaleghian, *Inorg. Chim. Acta* 461 (2017) 167.
- [67] A. H. Kianfar, W. A. K. Mahmood, M. Dinari, M. H. Azarian, F. Z. Khafri, *Spectrochim. Acta Part A* 127 (2014) 422.
- [68] A. Banerjee, S. Herrero, A. Gutiérrez, S. Chattopadhyay, *Polyhedron* 190 (2020) 114756.
- [69] M. Das, S. Chattopadhyay, *Polyhedron* 50 (2013) 443.
- [70] A. K. Maji, A. Chatterjee, S. Khan, B. K. Ghosh, R. Ghosh, *J. Mol. Struct.* 1146 (2017) 821.
- [71] S. M. Soliman, J. H. Albering, M. Farooq, M. A. M. Wadaan, A. El-Faham, *Inorg. Chim. Acta* 466 (2017) 16.
- [72] A. Datta, K. Das, C. Massera, J. K. Clegg, C. Sinha, J. -H. Huang, E. Garribba, *Dalton Trans.* 43 (2014) 5558.

- [73] D. G. Branzea, A. Guerri, O. Fabelo, C. Ruiz-Pérez, L.-M. Chamoreau, C. Sangregorio, A. Caneschi, M. Andruh, *Cryst. Growth Des.* 8 (2008) 941.
- [74] D. Aguila, L. A. Barrios, O. Roubeau, S. J. Teat and G. Aromi, *Chem. Commun.* 47 (2011) 707.
- [75] A. M. Madalan, H. W. Roesky, M. Andruh, M. Noltemeyer, N. Stanica, *Chem. Commun.* (2002) 1638.
- [76] J. -P. Costes, G. Novitchi, S. Shova, F. Dahan, B. Donnadieu, J. -P. Tuchagues, *Inorg. Chem.* 43 (2004) 7792.
- [77] S. K. Dey, A. Mukherjee, *Coord. Chem. Rev.* 310 (2016) 80.
- [78] A. Panja, *Polyhedron* 80 (2014) 81.
- [79] A. Panja, *Dalton Trans.* 43 (2014) 7760.
- [80] M. Das, B. N. Ghosh, A. Bauzá, K. Rissanen, A. Frontera, S. Chattopadhyay, *RSC Adv.* 5 (2015) 73028.
- [81] M. Mahato, D. Mondal, H. Nayek, *ChemistrySelect* 1 (2016) 6777.
- [82] A. Panja and P. Guionneau, *Dalton Trans.* 42 (2013) 5068.
- [83] A. Panja, N. C. Jana, P. Brandaõ, *New J. Chem.* 41 (2017) 9784.
- [84] A. Panja, M. Shyamal, A. Sahab, T. K. Mandal, *Dalton Trans.* 43 (2014) 5443.
- [85] A. Panja and A. Frontera, *Eur. J. Inorg. Chem.* (2018) 924.
- [86] K. Ghosh, K. Harms, S. Chattopadhyay, *Polyhedron* 123 (2017) 162.

[87] K. Ghosh, S. Roy, A. Ghosh, A. Banerjee, A. Bauzá, A. Frontera, S. Chattopadhyay, *Polyhedron* 112 (2016) 6.

[88] K. Ghosh, A. Banerjee, A. Bauzá, A. Frontera and S. Chattopadhyay, *RSC Adv.* 8 (2018) 28216.

[89] K. Ghosh, K. Harms, S. Chattopadhyay, *ChemistrySelect* 2 (2017) 8207.

Author contribution section

Abhisek Banerjee: He synthesized the complex and characterized it by spectral and elemental analysis and performed all necessary works.

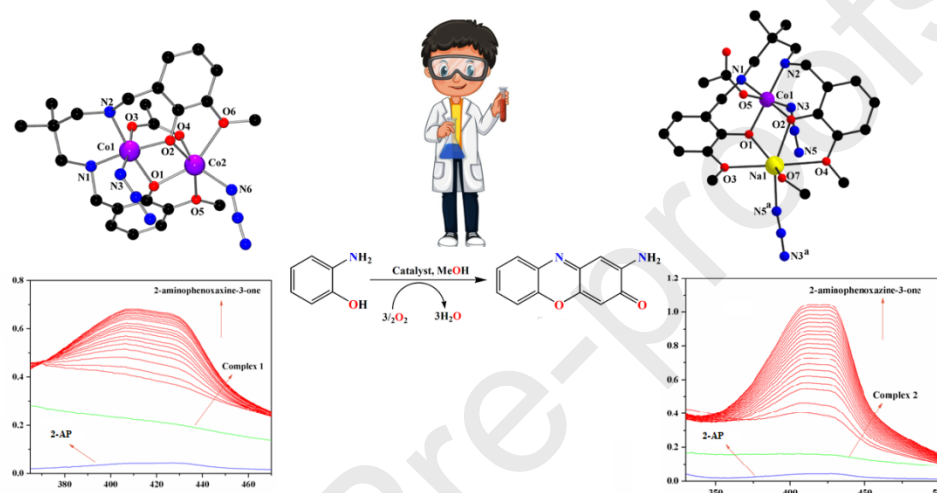
Shouvik Chattopadhyay: He is the Principal Investigator of the project. He is also the corresponding author.

Graphical Abstract

Dinuclear mixed valence cobalt(II/III) and hetero-tetranuclear cobalt(III)/Na complexes with a compartmental

ligand: Synthesis, characterization and use as catalysts for oxidative dimerisation of 2-aminophenol

Abhisek Banerjee, Shouvik Chattopadhyay*



A dinuclear mixed valence cobalt(III)/cobalt(II) complex and a tetranuclear cobalt(III)/sodium complex have been synthesized using a similar reduced Schiff base ligand under different reaction condition. Both complexes have been well characterized and they have the ability to show phenoxazinone synthase mimicking activity, which has been monitored spectrophotometrically.

Dinuclear mixed valence cobalt(II/III) and hetero-tetranuclear cobalt(III)/Na complexes with a compartmental ligand: Synthesis, characterization and use as catalysts for oxidative dimerisation of 2-aminophenol

Abhisek Banerjee, Shouvik Chattopadhyay*

Highlights

- Synthesis of a dinuclear mixed valence cobalt(II/III) complex and a hetero-tetranuclear cobalt(III)/Na complexes with a compartmental reduced Schiff base ligand.
- Confirmation of structures by single crystal X-ray diffraction.
- Exploration of their phenoxazinone synthase mimicking activity.